Influence of Acids and Alkalis on Transglycosylation and β-Elimination Pathway Kinetics during Cellulose Pyrolysis

Salim M. Shaik [a,b], C.Y. Koh [a], Paul Nicholas Sharratt [a] and Reginald B.H. Tan [a,b]

(a) Institute of Chemical and Engineering Sciences, 1, Pesek Road, Jurong Island, Singapore 627883, Singapore,
(b) Department of Chemical and Biomolecular Engineering, National University of Singapore, 21, Lower Kent Ridge Road, Singapore 119077, Singapore

Corresponding Author:

Salim M. Shaik: Institute of Chemical and Engineering Sciences,

1, Pesek Road, Jurong Island, Singapore 627883

Tel: (65)-6796-3950, Fax: (65)-6267-8835

E-mail: shaik_salim@ices.a-star.edu.sg

Abstract

The primary/initial thermal degradation pathways for the thermal degradation of cellulose are via intermolecular transglycosylation reactions within the glucose monomers of cellulose and via β-elimination (acid catalysed, heterolytic, ring-opening) reactions. Using the model-free isoconversional approach, the apparent activation energy of pure cellulose and cellulose that have been infused with acids (H_3PO_4, H_3BO_3) and alkalis ($Ba(OH)_2$, $Ca(OH)_2$) can be found.

We find that acids influence the thermal degradation by promoting the β-elimination pathway leading to more cellulose degrading via that route at the expense of transglycosylation. This manifests itself as an increase in the apparent activation energy of the overall cellulose pyrolysis. On the other hand, alkalis have a suppressing effect on the acid-catalysed β-elimination pathway which then allows more cellulose to degrade via transglycosylation. This seems to lower the apparent activation energy. Overall, we can see that the magnitude of the apparent activation energies are ordered as $E_{a,acid\text{-}cellulose} > E_{a,pure\text{-}cellulose} > E_{a,alkali\text{-}cellulose}$.

Keywords

Cellulose; Kinetics; Thermogravimetry; Pyrolysis; Transglycosylation; Levoglucosan.

1. Introduction

The main components of biomass are cellulose, hemicelluloses and lignin. In fact, cellulose is the most common form, making up half of the organic carbon on the planet. Hence, the cellulosic content of various biomass sources such as agricultural waste, municipal solid waste and microalgae plays an important role in the development of a sustainable feedstock for the production of renewable fuels and chemicals.

In their study of cellulose pyrolysis in the presence of flame retardants, Byrne et al. [1] observed that anhydrosaccharides were important intermediates in the degradation process. Following Madorsky et al. [2], Byrne and co-workers proposed that there were two main reaction routes. The first route involved intramolecular rearrangements that yielded anhydrosaccharides whilst the other route involved the formation of carbonium ions that decompose irreversibly (fragmentation). Based on the observations of two competing pathways for cellulose pyrolysis, Mamleev et al. [3] proposed a cellulose thermochemical conversion/pyrolysis scheme where the initial thermal degradation pathway is via intermolecular transglycosylation reactions within the glucose monomers of cellulose [3, 4]. Anhydrosaccharides (e.g. levoglucosan, levoglucosenone) are the primary products of this pathway. Alternatively, formation of liquid tar from cellulose can also occur via β-elimination. Under this mechanism, volatile acids (e.g. carboxylic acids) formed from the initial cellulose decomposition are able to attack the remaining cellulose as Bronsted acids thus catalysing heterolytic (ring-opening) reactions.

In addition to the hypothesised role of volatile acids in cellulose pyrolysis chemistry, it has also been known that acid or alkali content has a significant impact on the yields and product composition as shown by Budarin et al. [5] and Hassan et al. [6]. The levoglucosan yields of acid and alkaline treated biomass compared with untreated biomass are shown in Table 1. Although some of the results shown in Table 1 were conflicting, there seems to be some evidence that supports the hypothesis which suggests that acid catalysis would activate β-elimination whilst the presence of alkalis could suppress β-elimination and promote transglycosylation.

Mamleev et al. [7, 8] had also indicated that the acid-catalysed (β-elimination) pathway had a higher activation energy ($E_a \approx 250$ kJ/mol) compared with the transglycosylation pathway ($E_a \approx 200$ kJ/mol) during cellulose pyrolysis. These activation energy values were similar to those obtained by Capart et al. [9] in their study of pure cellulose decomposition

kinetics. Therefore, it follows that during thermal degradation, the apparent activation energy of acid infused cellulose should be closer to 250 kJ/mol (i.e. β-elimination dominated) whilst the apparent activation energy of alkali infused cellulose should be closer to 200 kJ/mol (i.e. transglycosylation dominated). In other words, the apparent thermal degradation activation energy of cellulose could be directly influenced to either increase or decrease by the presence of acids or alkalis within cellulose. Hence, the order of apparent activation energies should be: $\mathbf{E_{a,acid\text{-}cellulose} > E_{a,pure\text{-}cellulose} > E_{a,alkali\text{-}cellulose}}$.

This kinetics based approach would be useful in gaining further insights into the effects of acidic and alkaline additives. We would then be able to obtain further evidence with regards to the preference of either the β-elimination or transglycosylation pathways in the presence of acid and alkaline species. Consequently, the dominant pathway (transglycosylation or β-elimination) will result in a greater fraction of cellulose being thermally degraded via that route.

2. Experimental Section

Cellulose samples were prepared with different acid (H_3PO_4, H_3BO_3) and alkali ($Ba(OH)_2$, $Ca(OH)_2$) loadings by stirring microcrystalline cellulose (Avicel from Sigma-Aldrich) with the required acid (2, 3, 5wt%) or alkali (0.1, 0.5, 1wt%) solution at ca. 25°C for 30 minutes. The slurry was then filtered and dried overnight at 60°C. Thermogravimetric analyses were carried out with a TA Instruments SDT 2960 Simultaneous DSC-TGA. The system consists of a bifilar-wound furnace and a furnace tube enclosing two beams with platinum sensors at their ends where the sample and reference pans sit. Alumina pans with a volume of 90µl were used. For each test, the sample pan was loaded with 6 ± 0.05 mg of pure/treated cellulose sample and the reference pan was left empty. Nitrogen (flowrate = 200 ml/min) was used to purge the furnace tube throughout the test.

The thermal degradation was studied under non-isothermal conditions. The furnace temperature profile was programmed as follows:

i. linear increase at 5°C/min from ambient to 50°C: initial temperature ramp for sample drying
ii. isothermal at 50°C for 30 minutes: to ensure stability of sample prior to actual thermal analysis

iii. linear increase at various rates (2, 3, 4, 5 and 6°C/min) from 50°C to 650°C: non-isothermal thermal analysis region

iv. isothermal at 650°C for 10 minutes: end of thermal analysis.

Weight and temperature measurements were recorded from the DSC-TGA's micro-balance (sensitivity of 0.1µg) and thermocouple (ΔT sensitivity of 0.001°C) connected to the beams and processed via TA Universal Analysis software. The SDT 2960 was calibrated using three reference materials namely Tin (m.p. = 231.9 °C), Lead (m.p. = 327.5 °C) and Zinc (m.p. = 419.5 °C).

3. Kinetic Models for Cellulose Pyrolysis

The kinetics work found in the literature focussed mainly on obtaining the yields of the three main pyrolysis products namely char, tar and gas. In those studies, the lumped parameter approach to get the kinetic parameters, the char, tar and gas yields needed to be measured instantaneously (differential approach) [10, 11] or at the end of each experimental run (integral approach) [12-15]. The experimental data was then used to get the best-fitted kinetic parameters via a variety of non-linear regression methods/algorithms. This approach is however unsatisfactory if the compound(s) of interest are intermediates (e.g. levoglucosan, levoglucosenone) that are extremely difficult to isolate and measure temporally thus making the typical kinetic approach unsuitable.

Apart from the lumped parameter approach, kinetic parameters could be obtained via isothermal/non-isothermal thermogravimetric analysis (TGA). This evaluation of kinetic parameters by thermogravimetry can be conducted via model-free isoconversional method or via model-fitting.

3.1 Model-Free Isoconversional Method

This method requires the thermal decomposition to be carried out over a series of different heating rates. One of the biggest advantages of the isoconversional method is that the apparent activation energy could be determined without the need for a reaction model to be assumed or defined [16]. In addition, it is able to show the changes in activation energy as the reaction progresses.

The kinetics of cellulose thermal degradation or pyrolysis based on a single reaction, can be expressed in terms of mass conversion α by:

$$\frac{d\alpha}{dt} = k(T)f(\alpha) \quad (1)$$

Where $f(\alpha)$ is the reaction model and α is the conversion. The most common reaction model used is $f(\alpha)=1-\alpha$ (order one) although more recent literature have reported good fits using Nuclei-growth models (e.g. Avrami-Erofeev, Prout-Tompkins) [9, 17]. The temperature dependant rate constant, k, obeys the Arrhenius law: $k=A\exp(-E_a/RT)$. For the apparent activation energy E_a, a large variety of values were reported in literature which ranged from (100 to 250 kJ/mol) [7, 9, 17-20] with the higher values being more reliable according to Varhegyi et al. [21].

The conversion α is typically defined as:

$$\alpha = \frac{W_0 - W_t}{W_0 - W_f} \quad (2)$$

Where W_0, W_t and W_f are the sample weights initially, at time t and at the end of the experiment, respectively.

Several approaches have been developed for isoconversional methods which can be used for both isothermal and non-isothermal experimental data sets [22-27]. Of these, commonly used methods include the Flynn-Wall-Ozawa isoconversional method [28, 29] and the Friedman method [30, 31].

In the Friedman method, Equation (1) is rearranged to give:

$$\ln\left(\frac{\mathrm{d}\alpha}{\mathrm{d}t}\right)_i = \ln A + \ln[f(\alpha)] - \frac{E_\alpha}{RT_{\alpha,i}} \quad (3)$$

The activation energy E_α can therefore be evaluated by performing a series of thermogravimetric experiments at different heating rates. For a specific conversion α, the corresponding ($\mathrm{d}\alpha/\mathrm{d}t$) and temperature $T_{\alpha,i}$ can be obtained at the respective heating rates. A plot of $\ln\left(\frac{\mathrm{d}\alpha}{\mathrm{d}t}\right)$ against the reciprocal temperature should yield a straight line whose slope $\left(\frac{E_a}{R}\right)$ will provide the activation energy at that value of α. Repeating this procedure over a

range of α values will generate a profile of the variation of activation energy as the reaction progresses.

3.2 Model-fitting Method

The kinetic approach carried out by Capart et al. [9] is highly relevant in this study. Capart et al.[9] have shown that cellulose thermal degradation proceeds via two pathways similar to the β-elimination and transglycosylation reaction pathways. The reactions pathways were modelled after the Prout-Tompkins nuclei-growth model and can be generally expressed as follows:

$$\frac{dx_i}{dt} = -k_i x_i^{n_i}(1 - qx_i)^{m_i} \quad (4)$$

Where the unreacted fraction $x = (1 - \alpha)$, α = mass conversion, initiation parameter q = 0.99 for nucleation models, n = 0.5 or 1 for Prout-Tompkins model, m = acceleration parameter and $k = \mathrm{A}exp\left(\frac{-\mathrm{E}}{\mathrm{RT}}\right)$. Subsequently, Equation (4) can be specifically re-written as shown in Equation (5) and Equation (6) for the two cellulose thermal degradation pathways.

(Reaction 1, Transglycosylation) with n_1 =1, Prout-Tompkins:

$$\frac{dx_1}{dt} = -k_1 x_1(1 - 0.99x_1)^{m_1} \quad (5)$$

(Reaction 2, β-elimination) with m_2 =1 to ensure an induction time for generating volatiles from this pathway which is generally thought as the cracking route:

$$\frac{dx_2}{dt} = -k_2 x_2^{n_2}(1 - 0.99x_2) \quad (6)$$

Where: x_1 and x_2 are the cellulose fractions involved in Reactions 1 and 2 respectively and $x_1 = f_1 \times x$ and $x_2 = f_2 \times x$, where f_1 and f_2 are the fractions of the raw cellulose involved in Reactions 1 and 2 respectively.

Alternatively, the Prout-Tompkins model as expressed in Equation (5) will reduce to a first-order model when the acceleration parameter $m_1 = 0$ as shown in Equation (7). This greatly reduces the number of parameters that need to be fitted to just four (i.e. A_1, E_1, A_2, E_2)

$$\frac{dx_1}{dt} = -k_1 x_1 \tag{7}$$

Similarly, Equation (6) can also be reduced to a first order expression:

$$\frac{dx_2}{dt} = -k_2 x_2 \tag{8}$$

The unknown parameters namely A_1, E_1, m_1, f_1, A_2, E_2, n_2 and f_2 were evaluated by solving the ordinary differential equations (ODEs); equations (5) to (8) in MATLAB along with a genetic algorithm (GA) [32] as the optimiser for fitting the model parameters to the experimental results. The use of the genetic algorithm improves the likelihood of obtaining an optimum global solution to the model-fitting. This is in contrast to local optimisers than can get trapped at local minima thus providing only locally optimised solutions.

3.3 Kinetic Analysis of Acid/Alkali Infused Cellulose

To study the effects of acids and alkalis on cellulose thermal degradation, we will use both methods (model-free and model-fitting) in two stages as follows:

i. Stage 1: model-free, isoconversional method to evaluate apparent activation energy.
ii. Stage 2: model-fitting method to evaluate cellulose fraction thermally degraded by dominant pathway (transglycosylation or β-elimination).

In the first stage, the model-free, isoconversional approach was selected because the activation energy evaluated would otherwise be affected by variations being force-fitted or hidden within the reaction model parameters. Out of the several isoconversional methods available, the Friedman method was selected for use due to its utility and recommendations in recent publications [33, 34].

In the second stage, the models (nucleation and first-order) as described by equation (5) to (8) are known in literature. The models were then used to study the effects of acid and alkali

additives on the hypothesised pathways (i.e. transglycosylation and β-elimination) based on the non-isothermal TGA data that have been obtained.

4. Results and Discussion

Thermal analysis using the DSC-TGA was first carried out on pure, untreated microcrystalline cellulose samples at the various heating rates. This was done to compare our results with literature values and verify the compatibility of our instrument and techniques. The activation energy for pure cellulose using Friedman's isoconversional method was then calculated and found to be 203 ± 13 kJ/mol (at 95% confidence limit). This was very close to the values obtained by Capart et al. [9] which obtained activation energies of 203 kJ/mol (isothermal mode) and 200 kJ/mol (non-isothermal mode).

4.1 Conversion Rate Profiles of Cellulose Degradation

Similar experiments and analysis were then carried out for cellulose samples that were infused with acids (H_3PO_4, H_3BO_3) and alkalis ($Ba(OH)_2$, $Ca(OH)_2$). An analysis of the cellulose degradation rates as expressed by ($d\alpha/dt$) against the progress of the reaction indicated by conversion α is useful in determining the presence of multiple reactions. It will also help us in determining the starting and ending points of the main thermal degradation reaction(s). The typical conversion profiles of the acid and alkali infused cellulose are shown in Figures 1 to 4.

Based on these profiles, a few observations can be made. Firstly, for the two acids, it can be seen that the main thermal degradation reaction terminates when the conversion α = 0.4. It is likely that a second reaction is occurring when $0.4 < \alpha < 0.8$. On the other hand, for the alkalis, the thermal degradation profiles were consistently smooth suggesting that there was a single primary reaction throughout conversion levels from $\alpha = 0$ to $\alpha = 0.7$. Hence, for the evaluation of activation energy, with respect to the initial transglycosylation and β-elimination pathways, we will only consider the values of $0 < \alpha < 0.4$ for the acid infused cellulose while for the alkalis, we will evaluate in the region $0 < \alpha < 0.7$.

4.2 Effect of Acids on Activation Energy

We can see in Figure 5 that the activation energy for H_3PO_4 is clustered closely around the 250 kJ/mol level. Meanwhile, in Figure 6, the activation energy scatter for H_3BO_3 infused cellulose seems to be more widely distributed although most seem to still cluster close to the 250 kJ/mol level. The mean values are seen to range from ca. 310 kJ/mol to as low as ca. 220 kJ/mol. The mean values of activation energies for all the acid treated samples were calculated and are presented in Table 2.

The activation energy values were tested using a one-sample t-test. The null hypothesis was set as the mean activation energy $E_a = 250$ kJ/mol whilst the alternative hypothesis was set as the activation energy $E_a \neq 250$ kJ/mol. At a significance level of 0.05, four five out of the six samples analysed had have means that were are not significantly different from an activation energy level $E_a = 250$ kJ/mol. Meanwhile, the remaining samples had means $E_a = 240$ kJ/mol andis 255 kJ/mol (at 0.05 significance level). A complementary t-test was also conducted and it shows that all the samples means are significantly higher than the activation energy $E_a = 200$ kJ/mol (at 0.05 significance level). This shift of the activation energy to ca. 250 kJ/mol is close to the expected activation energy of 250 kJ/mol for the β-elimination pathway.

4.3 Effect of Alkalis on Activation Energy

Similar to the analysis done for the acid samples, the activation energies for alkalis ($Ba(OH)_2$, $Ca(OH)_2$) were calculated using Friedman's method and presented as isoconversion plots in Figure 7 and Figure 8 respectively.

In contrast to the acid infused cellulose plots which cluster mainly at the 250 kJ/mol level, the alkali infused samples show clustering at or just below the 200 kJ/mol level. Overall, the plots are seen to more consistent than the acid infused cellulose plots which is to be expected due to the smoother conversion rate plots shown in Figure 3 and Figure 4.

When the respective mean activation energies were calculated (see Table 2), it can be seen that the values are significantly less than the values obtained for the acid treated cellulose samples. In fact, they seem to be consistently below the 200 kJ/mol level as was initially expected for transglycosylation reaction. This is confirmed by the statistics obtained for the t-test. However, it can be clearly seen that all the activation energies for alkali infused cellulose were significantly lower than those for acids. This shift of the activation energy to

ca.180 kJ/mol is lower than the expected activation energy of 200 kJ/mol for the transglycosylation pathway. This could be partially due to potential secondary effects of the alkali cations. It does however provide evidence that the β-elimination pathway is suppressed.

4.4. Dominant Pathway for Pure Cellulose Degradation

Model-fitting was carried out using MATLAB based on the ODEs expressed in equations (5) to (8) at different heating rates. The model parameters used initially were as stipulated in Capart et al. [9] with m_1=0.481, f_1=0.75, A_1=1.94x10^{15} 1/s, E_1=202.65 kJ/mol, n_2=22, f_2=0.163, A_2=1.63x10^{20} 1/s and E_2=255 kJ/mol . The results of the simulated cellulose thermal degradation using Capart's model are shown in Figure 9. As can be seen in the plots, the Capart model does not seem to fit the experimental cellulose thermal degradation data that we have obtained. However, qualitatively, the overall shape of Capart's model curves is consistent with the experiment data.

We then freed the constraints on Capart's model parameters and allowed MATLAB to optimise the parameters using the in-built genetic algorithm. The fitted model parameters obtained from this optimisation process are n_1=1.0, m_1=6.6x10^{-5}, n_2=1.0, m_2=0.02. These values practically collapse the nuclei-growth model into a first-order reaction model as described by equation (7) and equation (8). We then proceeded with fitting the experimental data with this first-order model and obtained good fits as shown in Figure 10. The Arrhenius parameters for the first-order model are: A_1=1.5x10^{15} s^{-1}, E_1=203 kJ/mol, A_2=2.0x10^{19} 1/s, E_2=257 kJ/mol. Based on this first-order model, the amount of intermediates generated from transglycosylation and β-elimination was found. The final level of these intermediates gives an indication of the fraction of cellulose that degraded along each of the pathway.

The activation energies obtained are generally consistent with the expected values for the two pathways. We are also able to observe that the fraction of cellulose thermally degraded via transglycosylation is greater than that via β-elimination as evidenced by f_1 and f_2 values respectively. The fraction of cellulose that underwent thermal degradation via transglycosylation pathway varies from 0.42 to 0.67 with the fraction increasing with increasing heating rates. The pathway degradation ratio (PDR) f_1:f_2 ranged from 1:1 to 3.5:1.

This provides an indication that transglycosylation is the dominant pathway for pure cellulose thermal degradation/pyrolysis especially at higher heating rates.

Increasing the heating rates of fast pyrolysis has been shown by many workers including recently by Hoekstra et al. [35] to increase bio-oil yields. In addition, it has been reported in literature that anhydrosaccharides especially levoglucosan is a major component of fast pyrolysis bio-oils [36-38]. These observations suggest that heating rates can affect the pathway through which cellulose degrades. Based on the TGA fits that we have obtained, the predominance of the transglycosylation pathway is likely the reason why more levoglucosan is produced at higher heating rates. This preference for transglycosylation rather than β-elimination could be explained by the presence or lack thereof of volatile organic acids which are secondary products of cellulose pyrolysis. It was observed that the yields of levoglucosan can also be increased when cellulose is pyrolysed under vaccum [39]. Here, the organic acids are volatilised to a greater degree under vacuum thereby decreasing their ability to catalyse the β-elimination route.

A similar argument can be proposed for the heating rates in that at lower heating rates, cellulose is kept within lower temperature regions for a longer period of time than at high heating rates. This in turn allows the volatile organic acids to remain within the cellulose sample for longer periods and catalyse the β-elimination pathway. These acids could also contribute to increased char levels seen at lower heating rates.

The first-order model that was successfully used for pure cellulose was then applied to the acid (H_3PO_4 and H_3BO_3) and alkali ($Ba(OH)_2$ and $Ca(OH)_2$) infused cellulose samples.

4.5. Dominant Pathway for Acid Infused Cellulose Degradation

The comparison plots of the first-order simulation results and experimental TGA data for 2 wt% H_3PO_4 infused cellulose degradation are shown in Figure 11 while the detailed kinetic results from all the H_3PO_4 infused cellulose are listed in Table 3.

From a qualitative point of view, the first-order model seems to be able to provide an adequate fit for the experimental results. The fit is better in the initial stages compared to the latter stages of thermal degradation as seen from the deviation when the fraction of unreacted cellulose x is less than 0.6 (i.e. conversion $\alpha > 0.4$). The experimental data points indicated a

decrease in degradation rate towards the end. This could be explained by the dα/dt plots shown in Figures 1 and 2 which showed that the primary degradation rate curves ended around those points. What we can therefore say is that the transglycosylation and β-elimination pathways were the dominant reactions in the early part of cellulose degradation which is then followed by other secondary reactions (e.g. cracking to other lighter organics). This was shown by Mamleev et al. [7] in that it was observed that the relationship between activation energy and conversion α had "two pronounced plateaus" that corresponded with an initial primary degradation pathway that is then followed by secondary reactions that became dominant. These observations also find support in the recent work by Vinu and Broadbelt [40], their quantum chemistry calculations and modelling were able to give reasonable predictions of levoglucosan but significant deviations from experimental results were observed when predicting the yields of light organics such as formic acid and glycoaldehyde. They have attributed this to secondary reactions not considered by their model.

The overall goodness of fit for the first-order model as expressed by R^2 was greater than 0.92 and can be generally thought to be reasonable with the understanding that the kinetic parameters obtained to be representative only of the initial part of the thermal degradation process where the initial cellulose degradation pathways (transglycosylation and β–elimination) are dominant. The original Capart model as defined by equations (5) and (6) were also used in trials to fit the experimental data with goodness-of-fit values of R^2 ranging from 0.77 to 0.80. Therefore only the results from the first-order model were used in the subsequent pathway analysis.

The results in Table 3 also show that the mean activation energy for transglycosylation pathway, $E_{1,ave}$ is 199 kJ/mol whilst for β-elimination, the mean activation energy $E_{2,ave}$ is 255 kJ/mol. These values are similar to the activation energy results for pure cellulose (literature and current work). More significantly, we note that the fraction of cellulose involved in β-elimination (f_2) was higher than the fraction for transglycosylation (f_1). The pathway degradation ratio (PDR) f_1:f_2 ranged from 1:2.5 to 1:5. This is a reversal from the results that we obtained for pure cellulose. It is also indicative of the β-elimination pathway being dominant during the thermal degradation of H_3PO_4 infused cellulose.

Thermal degradation/pyrolysis data of H_3BO_3 infused cellulose was subjected to the same analysis and the model-fitting plots are presented in Figure 12. The fitting of the first-

order model to the experimental results obtained for the various levels of H_3BO_3 loadings yielded the kinetic parameters as listed in Table 3.

Generally, we obtain similar results for the H_3BO_3 infused cellulose when comparing with the earlier H_3PO_4 infused cellulose results. For the transglycosylation pathway, the mean activation energy, $E_{1,ave}$ is 204 kJ/mol whilst for the β-elimination pathway, $E_{2,ave}$ is 260 kJ/mol. These values are also similar to the activation energy results for pure cellulose. The fraction of cellulose showed a trend of favouring β-elimination rather than transglycosylation. This is reflected in the PDR (f_1:f_2) which ranged from 1:0.8 to 1:1.7. Although there also seems to be a shift in dominance from transglycosylation to β-elimination, this shift is not as large as the one we observe for the H_3PO_4 loadings. However, we can still see that this is still indicative of the β-elimination pathway becoming more dominant during the thermal degradation of H_3BO_3 infused cellulose.

4.6 Dominant Pathway for Alkali Infused Cellulose Degradation

To compare and contrast the results we obtained for the acid infused cellulose, similar model fitting and analysis were carried out for the thermal degradation of $Ba(OH)_2$ infused cellulose. The model-fitting plots are shown in Figure 13 for 0.1 wt% $Ba(OH)_2$ infused cellulose. The detailed kinetic results for all the different alkali loadings are shown in Table 3.

Generally, the first-order model fitted the $Ba(OH)_2$ experimental value rather well (R^2>0.94). Fittings were also attempted using the Capart model as described by equations (5) and (6) but the goodness of fit (R^2) obtained were less than 0.93. Therefore, the subsequent pathway analysis was conducted based on the first-order model. As with the acid loadings, there still seemed to be a deviation towards the later stages of thermal degradation. However, this deviation occurred later when the fraction of unreacted cellulose $x < 0.2$ compared to $x <$ 0.6 for the acid infused cellulose. The transglycosylation pathway was found to have a mean activation energy $E_{1,ave}$= 203 kJ/mol whilst for β-elimination, the mean activation energy $E_{2,ave}$ = 260 kJ/mol. These values are close to the literature values and to the ones obtained for pure cellulose. The fraction of cellulose involved in transglycosylation (f_1) was much higher than those obtained for the acid loadings. The PDR (f_1:f_2) for $Ba(OH)_2$ loadings ranged from 3:1 to 5.4:1. Overall, these values indicate that transglycosylation is the likely dominant

pathway, and the values are greater than the PDR (f_1:f_2) range for pure cellulose. This would suggest that the alkalis affect cellulose pyrolysis by neutralising the organic acids produced during pyrolysis thus suppressing the β-elimination pathway.

The model fittings for 0.1 wt% $Ca(OH)_2$ infused cellulose as shown in Figure 14, are generally acceptable (R^2>0.93) and comparable with those obtained earlier for pure cellulose and $Ba(OH)_2$. Consequently, the relevant kinetic parameters were found from the model fittings and are tabulated in Table 3. The mean activation energy for transglycosylation was 200 kJ/mol whilst the mean activation energy for β-elimination was 257 kJ/mol. These values are comparable to the ones that have been obtained for pure cellulose, acid infused cellulose and $Ba(OH)_2$. In terms of pathway degradation fraction, it is observed that f_1 (transglycosylation) was greater than f_2 (β-elimination). This showed that transglycosylation was the dominant pathway with the PDR (f_1:f_2) lying between 2.3:1 and 4.7:1.

5. Conclusion

Overall we can see that the presence of acids and alkalis have a significant effect on the kinetics of cellulose thermal degradation or pyrolysis. Acids are able to raise the apparent activation energy of cellulose thermal degradation whilst alkalis are able to decrease the apparent activation energy. The results show that:

$$\mathbf{E_{a,acid\text{-}cellulose} > E_{a,pure\text{-}cellulose} > E_{a,alkali\text{-}cellulose}}.$$

The apparent activation energy of cellulose degradation obtained via the isoconversional method is based on describing the conversion as a single step, single pathway degradation. However, as hypothesised, this degradation actually comprise of two main competitive reactions (i.e. transglycosylation and β-elimination). When this is taken into consideration, we can see that the activation energies of the two pathways were found to be on average 202 kJ/mol (transglycosylation) and 258 kJ/mol (β-elimination) for the various acids and alkalis infused cellulose. These activation energy values are consistent with the findings of Mamleev et al.[3].

Instead of activation energy shifts, we can now see that the acidic/alkaline additives manifest their influence via changes in the fraction of cellulose degraded via the two pathways. Acids influence the thermal degradation by promoting the β-elimination pathway

which leads to more cellulose degrading via that route at the expense of transglycosylation. This had manifested itself earlier as an increase in the apparent activation energy. On the other hand, alkalis have a suppressing effect on the acid-catalysed β-elimination pathway which then allows more cellulose to degrade via transglycosylation. This was seen as a lowering of the apparent activation energy found via the isoconversional method.

In terms of modelling acid/alkali infused cellulose thermal degradation, we see that there was a greater deviation between the first-order model prediction and the experimental TGA results towards the later stages. It is likely that secondary reactions instead of transglycosylation or β-elimination are dominant in these regions. There is therefore a need to further elucidate the reaction network in detail beyond the initial transglycosylation and β-elimination pathways. Concurrently, we would also need to identify and study all the reaction intermediates and their interactions with H^+ and OH^- ions in order to develop a better overall model for cellulose pyrolysis.

The findings thus far naturally lead to the idea that we might be able to selectively increase the yields of anhydrosaccharides which are only formed via the transglycosylation pathway. This could be achieved by controlling or manipulating the acidity/alkalinity of the environment in which cellulose thermally degrades or pyrolyses. Although the use of alkalis show the possibility of increasing anhydrosaccharide yields, the presence of alkali cations seem to have a negative effect on the overall yields. Therefore process schemes that could remove H^+ ions without the need to introduce cations might prove to be more beneficial and should be studied.

Acknowledgements

Funding for this work was provided by the Agency for Science, Technology & Research (A-STAR) Singapore via the Bioenergy Thematic Programme.

Nomenclature

α	conversion
A	Arrhenius pre-exponent factor, 1/s
A_1	Arrhenius pre-exponent factor (transglycosylation), 1/s
A_2	Arrhenius pre-exponent factor (β-elimination), 1/s
E_1	activation energy (transglycosylation) , kJ/mol
$E_{1,ave}$	mean activation energy (transglycosylation) , kJ/mol
E_2	activation energy (β-elimination) , kJ/mol
$E_{2,ave}$	mean activation energy (β-elimination) , kJ/mol
E_a	apparent activation energy
E_α	activation energy at a specific conversion α
$f(\alpha)$	reaction model
f_1	fraction of the raw cellulose involved in Reaction 1 (transglycosylation)
f_2	fraction of the raw cellulose involved in Reaction 2 (β-elimination)
k	Arrhenius rate constant, 1/s
m	acceleration parameter for Prout-Tompkins model
m.p.	melting point
n	exponent parameter for Prout-Tompkins model
q	initiation parameter
R	gas constant, J/K mol
T	temperature, Kelvin (K)
W_0	sample weight at time=0
W_f	sample weight at the end
W_t	sample weight at time=t
x	unreacted fraction

References

[1] G.A. Byrne, D. Gardiner, F.H. Holmes, The pyrolysis of cellulose and the action of flame-retardants, J. Appl. Chem., 16 (1966) 81-88.
[2] S.L. Madorsky, V.E. Hart, S. Straus, Pyrolysis of Cellulose in a Vacuum, J. Res. Natl. Bur. Stand., 56 (1956) 343.
[3] V. Mamleev, S. Bourbigot, M.L. Bras, J. Yvon, The facts and hypotheses relating to the phenomenological model of cellulose pyrolysis. Interdependence of the steps, J. Anal. Appl. Pyrolysis, 84 (2009) 1-17.
[4] R.G. Graham, B.A. Bergougnou, R.P. Overend, Fast pyrolysis of biomass, J. Anal. Appl. Pyrolysis, 6 (1984) 95-135.
[5] V.L. Budarin, J.H. Clark, B.A. Lanigan, P. Shuttleworth, S.W. Breeden, A.J. Wilson, D.J. Macquarrie, K. Milkowski, J. Jones, T. Bridgeman, A. Ross, The preparation of high grade bio-oils through the controlled, low temperature microwave activation of wheat straw, Bioresour. Technol., 100 (2009) 6064-6068.
[6] E.M. Hassan, P.H. Steele, L. Ingram, Characterization of fast pyrolysis bio-oils produced from pretreated pine wood, Appl. Biochem. Biotechnol., 154 (2009) 3-13.
[7] V. Mamleev, S. Bourbigot, J. Yvon, Kinetic analysis of the thermal decomposition of cellulose: The change of the rate limitation, J. Anal. Appl. Pyrolysis, 80 (2007) 141-150.
[8] V. Mamleev, S. Bourbigot, J. Yvon, Kinetic analysis of the thermal decomposition of cellulose: The main step of mass loss, J. Anal. Appl. Pyrolysis, 80 (2007) 151-165.
[9] R. Capart, L. Khezami, A.K. Burnham, Assessment of various kinetic models for the pyrolysis of a microgranular cellulose, Thermochim. Acta, 417 (2004) 79-89.
[10] J.L. Banyasz, S. Li, J. Lyons-Hart, K.H. Shafer, Gas evolution and the mechanism of cellulose pyrolysis, *Fuel*, 80 (2001) 1757-1763.
[11] M.G. Gronli, M.C. Melaaen, Mathematical Model for Wood PyrolysisComparison of Experimental Measurements with Model Predictions, Energy Fuels, 14 (2000) 791-800.
[12] M.R. Hajaligol, J.B. Howard, J.P. Longwell, W.A. Peters, Product compositions and kinetics for rapid pyrolysis of cellulose, Ind. Eng. Chem. Process Des. Dev., 21 (1982) 457-465.
[13] T.R. Nunn, J.B. Howard, J.P. Longwell, W.A. Peters, Product compositions and kinetics in the rapid pyrolysis of milled wood lignin, Ind. Eng. Chem. Process Des. Dev., 24 (1985) 844-852.
[14] D.S. Scott, J. Piskorz, D. Radlein, Liquid products from the continuous flash pyrolysis of biomass, Ind. Eng. Chem. Process Des. Dev., 24 (1985) 581-588.
[15] C. Sheng, J.L.T. Azevedo, Modeling biomass devolatilization using the chemical percolation devolatilization model for the main components, Proc. Combust. Inst., 29 (2002) 407-414.
[16] S. Vyazovkin, C.A. Wight, Model-free and model-fitting approaches to kinetic analysis of isothermal and nonisothermal data, Thermochim. Acta, 340–341 (1999) 53-68.
[17] H. Barud, C. Ribeiro, J. Capela, M. Crespi, S. Ribeiro, Y. Messadeq, Kinetic parameters for thermal decomposition of microcrystalline, vegetal, and bacterial cellulose, J. Therm. Anal. Calorim., 105 (2011) 421-426.
[18] M. Gronli, M.J. Antal, G. Varhegyi, A Round-Robin Study of Cellulose Pyrolysis Kinetics by Thermogravimetry, Ind. Eng. Chem. Res., 38 (1999) 2238-2244.

[19] I. Milosavljevic, E.M. Suuberg, Cellulose Thermal Decomposition Kinetics: Global Mass Loss Kinetics, Ind. Eng. Chem. Res., 34 (1995) 1081-1091.
[20] M. Poletto, V. Pistor, M. Zeni, A.J. Zattera, Crystalline properties and decomposition kinetics of cellulose fibers in wood pulp obtained by two pulping processes, Polym. Degrad. Stab., 96 (2011) 679-685.
[21] G. Varhegyi, M.J. Antal, T. Szekely, P. Szabo, Kinetics of the thermal decomposition of cellulose, hemicellulose, and sugarcane bagasse, Energy Fuels, 3 (1989) 329-335.
[22] M.E. Brown, M. Maciejewski, S. Vyazovkin, R. Nomen, J. Sempere, A. Burnham, J. Opfermann, R. Strey, H.L. Anderson, A. Kemmler, R. Keuleers, J. Janssens, H.O. Desseyn, C.-R. Li, T.B. Tang, B. Roduit, J. Malek, T. Mitsuhashi, Computational aspects of kinetic analysis: Part A: The ICTAC Kinetics Project-data, methods and results, Thermochim. Acta, 355 (2000) 125-143.
[23] A.K. Burnham, Computational aspects of kinetic analysis: Part D: The ICTAC Kinetics Project-multi-thermal-history model-fitting methods and their relation to isoconversional methods, Thermochim. Acta, 355 (2000) 165-170.
[24] M. Maciejewski, Computational aspects of kinetic analysis: Part B: The ICTAC Kinetics Project-the decomposition kinetics of calcium carbonate revisited, or some tips on survival in the kinetic minefield, Thermochim. Acta, 355 (2000) 145-154.
[25] B. Roduit, Computational aspects of kinetic analysis: Part E: The ICTAC Kinetics Project-numerical techniques and kinetics of solid state processes, Thermochim. Acta, 355 (2000) 171-180.
[26] S. Vyazovkin, Computational aspects of kinetic analysis: Part C: The ICTAC Kinetics Project-the light at the end of the tunnel?, Thermochim. Acta, 355 (2000) 155-163.
[27] J. Farjas, P. Roura, Isoconversional analysis of solid state transformations, J. Therm. Anal. Calorim., 105 (2011) 757-766.
[28] J.H. Flynn, L.A. Wall, General treatment of the thermogravimetry of polymers, J. Res. Natl. Bur. Stand., Sect. A, 70A (1966) 487-523.
[29] T. Ozawa, Kinetic analysis of derivative curves in thermal analysis, J. Therm. Anal. Calorim., 2 (1970) 301-324.
[30] H.L. Friedman, Kinetics of thermal degradation of char-forming plastics from thermogravimetry. Application to a phenolic plastic, J. Polym. Sci., Part C: Polym. Symp., 6 (1964) 183-195.
[31] H.L. Friedman, Kinetics and Gaseous Products of Thermal Decomposition of Polymers, J. Macromol. Sci., Part A: Pure Appl.Chem., 1 (1967) 57-79.
[32] A.J. Chipperfield, P.J. Fleming, The MATLAB Genetic Algorithm Toolbox, IEE Seminar Digests, 1995 (1995) 10-10.
[33] P.E. Sanchez-Jimenez, L.A. Perez-Maqueda, A. Perejon, J. Pascual-Cosp, M. Benitez-Guerrero, J.M. Criado, An improved model for the kinetic description of the thermal degradation of cellulose, Cellulose, 18 (2011) 1487-1498.
[34] T. Vlase, G. Vlase, N. Birta, N. Doca, Comparative results of kinetic data obtained with different methods for complex decomposition steps, J. Therm. Anal. Calorim., 88 (2007) 631-635.
[35] E. Hoekstra, W.P.M. Van Swaaij, S.R.A. Kersten, K.J.A. Hogendoorn, Fast pyrolysis in a novel wire-mesh reactor: Decomposition of pine wood and model compounds, Chem. Eng. J., 187 (2012) 172-184.
[36] Q. Li, P.H. Steele, F. Yu, B. Mitchell, E.-B.M. Hassan, Pyrolytic spray increases levoglucosan production during fast pyrolysis, J. Anal. Appl. Pyrolysis, 100 (2013) 33-40.
[37] D.S. Scott, J. Piskorz, D. Radlein, P. Majerski, Process for the production of anhydrosugars and fermentable sugars from fast pyrolysis liquids, in, 1997.

[38] F. Shafizadeh, R.H. Furneaux, T.G. Cochran, J.P. Scholl, Y. Sakai, Production of levoglucosan and glucose from pyrolysis of cellulosic materials, J. Appl. Polym. Sci., 23 (1979) 3525-3539.
[39] G.-J. Kwon, D.-Y. Kim, S. Kimura, S. Kuga, Rapid-cooling, continuous-feed pyrolyzer for biomass processing: Preparation of levoglucosan from cellulose and starch, , J. Anal. Appl. Pyrolysis, 80 (2007) 1-5.
[40] R. Vinu, L.J. Broadbelt, A mechanistic model of fast pyrolysis of glucose-based carbohydrates to predict bio-oil composition, Energy Environ. Sci., 5 (2012) 9808-9826.

Table1

Table 1: Comparison of the effects of acids and alkalis on biomass pyrolysis yields.

	Budarin et al.			**Hassan et al.**				
additives	H_2SO_4	HCl	NH_3	H_3PO_4	H_2SO_4	NaOH	$Ca(OH)_2$	NH_4OH
levoglucosan	↓ 26%	↑ 27%	↑ 66%	↓ 54%	↓ 61%	↓ 49%	↑ 72%	↑ 41%

Table2

Table 2: Average activation energy of cellulose with the various acid and alkaline additives

	2 wt% H_3PO_4	3 wt% H_3PO_4	5 wt% H_3PO_4
E_a(kJ/mol)	249 ± 9	247 ± 12	239 ± 6
	2 wt% H_3BO_3	3 wt% H_3BO_3	5 wt% H_3BO_3
E_a(kJ/mol)	252 ± 26	258 ± 26	268 ± 15
	0.1 wt% $Ba(OH)_2$	0.5 wt% $Ba(OH)_2$	1 wt% $Ba(OH)_2$
E_a(kJ/mol)	181 ± 5	178 ± 3	184 ± 2
	0.1wt% $Ca(OH)_2$	0.5wt% $Ca(OH)_2$	1 wt% $Ca(OH)_2$
E_a(kJ/mol)	183 ± 5	198 ± 2	194 ± 6

Table3

Table 3: Fitted model parameters obtained for first-order thermal degradation model – H_3PO_4, H_3BO_3, $Ba(OH)_2$, $Ca(OH)_2$ impregnated cellulose

	Transglycosylation			**β-Elimination**		
	A_1 (1/s)	**E_1 (kJ/mol)**	***f_1***	**A_2 (1/s)**	**E_2 (kJ/mol)**	***f_2***
Cellulose + 2wt% H_3PO_4	$6.68x10^{15}$	204	0.17	$3.30\ x10^{21}$	260	0.53
Cellulose + 3wt% H_3PO_4	$7.30x10^{15}$	191	0.09	$7.68\ x10^{21}$	244	0.41
Cellulose + 5wt% H_3PO_4	$6.46x10^{15}$	203	0.18	$5.10\ x10^{21}$	261	0.52
Cellulose + 2wt% H_3BO_3	$1.46x10^{15}$	204	0.41	$1.10\ x10^{20}$	260	0.36
Cellulose + 3wt% H_3BO_3	$1.46x10^{15}$	204	0.37	$1.10\ x10^{20}$	260	0.38
Cellulose + 5wt% H_3BO_3	$1.46x10^{15}$	203	0.30	$2.70\ x10^{20}$	260	0.44
Cellulose + 0.1wt% $Ba(OH)_2$	$1.46x10^{15}$	208	0.76	$1.02\ x10^{19}$	260	0.17
Cellulose + 0.5wt% $Ba(OH)_2$	$3.30x10^{14}$	201	0.72	$1.01\ x10^{19}$	261	0.19
Cellulose + 1wt% $Ba(OH)_2$	$3.30x10^{14}$	201	0.68	$1.01\ x10^{19}$	260	0.20
Cellulose + 0.1wt% $Ca(OH)_2$	$4.00x10^{14}$	200	0.71	$1.07\ x10^{19}$	257	0.23
Cellulose + 0.5wt% $Ca(OH)_2$	$4.93x10^{14}$	200	0.74	$1.07\ x10^{19}$	257	0.18
Cellulose + 1wt% $Ca(OH)_2$	$4.10x10^{14}$	201	0.64	$1.07\ x10^{19}$	257	0.24

Figure1

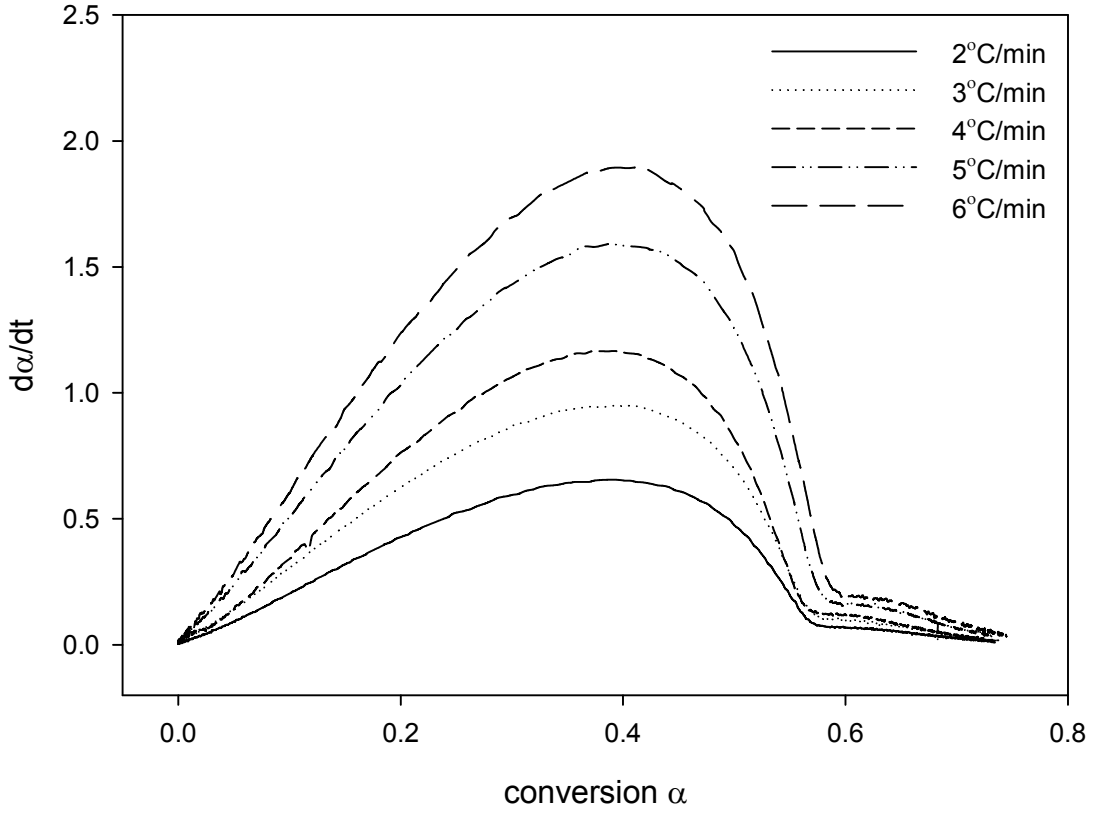

Figure 1: Variation of conversion rate (dα/dt) for cellulose impregnated with 5wt% H_3PO_4 at various TGA heating rates (2-6 °C/min).

Figure2

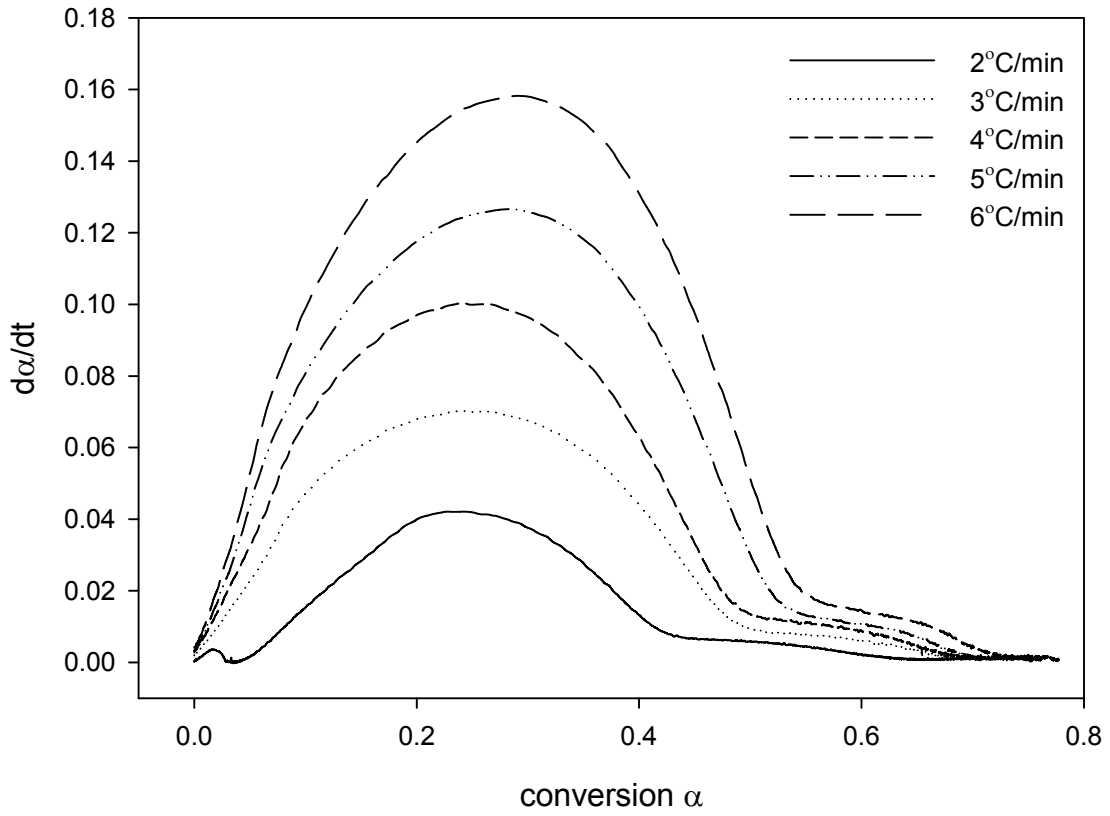

Figure 2: Variation of conversion rate (dα/dt) for cellulose impregnated with 5wt% H_3BO_3 at various TGA heating rates (2-6 °C/min).

Figure3

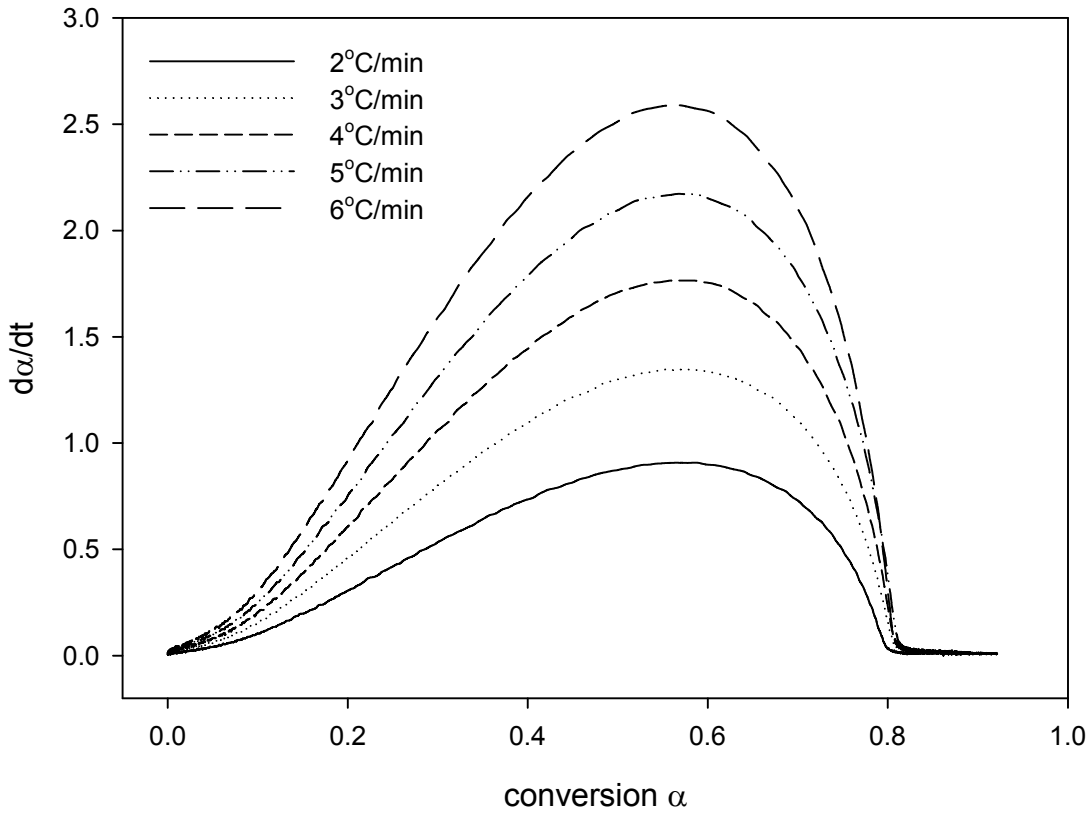

Figure 3: Variation of conversion rate (dα/dt) for cellulose impregnated with 1wt% $Ba(OH)_2$ at various TGA heating rates (2-6 °C/min)

Figure4

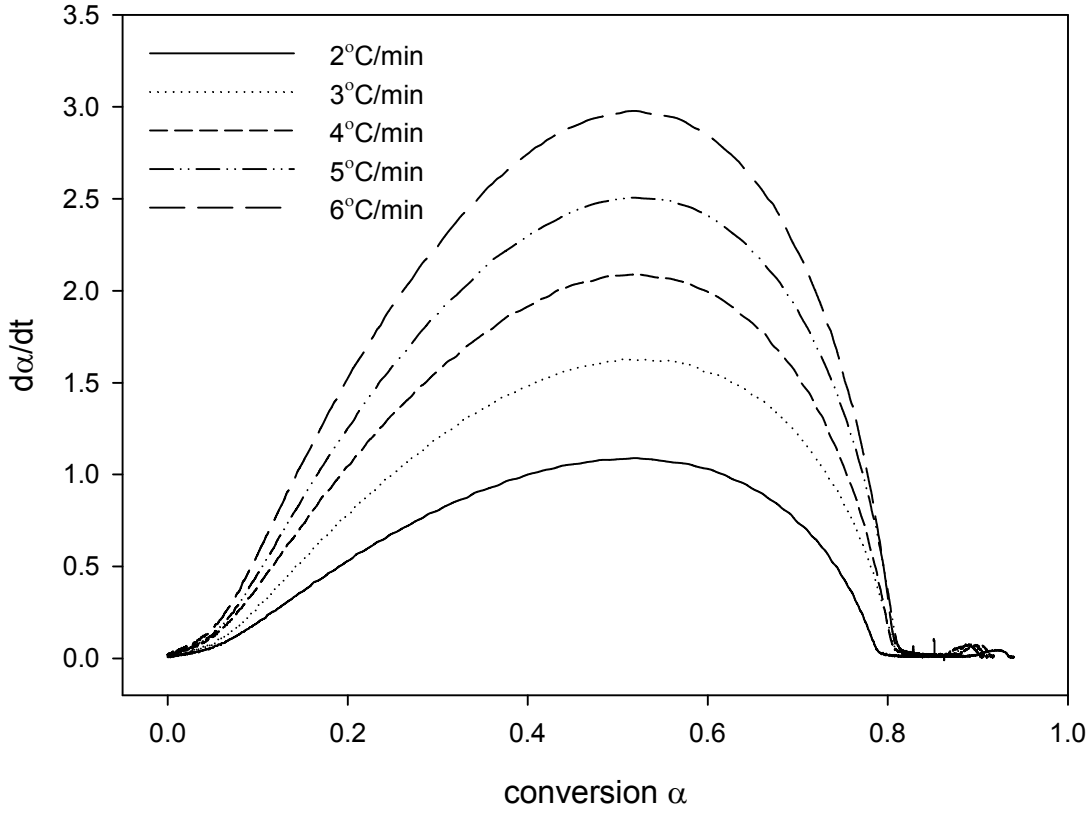

Figure 4: Variation of conversion rate (dα/dt) for cellulose impregnated with 1wt% $Ca(OH)_2$ at various TGA heating rates (2-6 °C/min)

Figure5

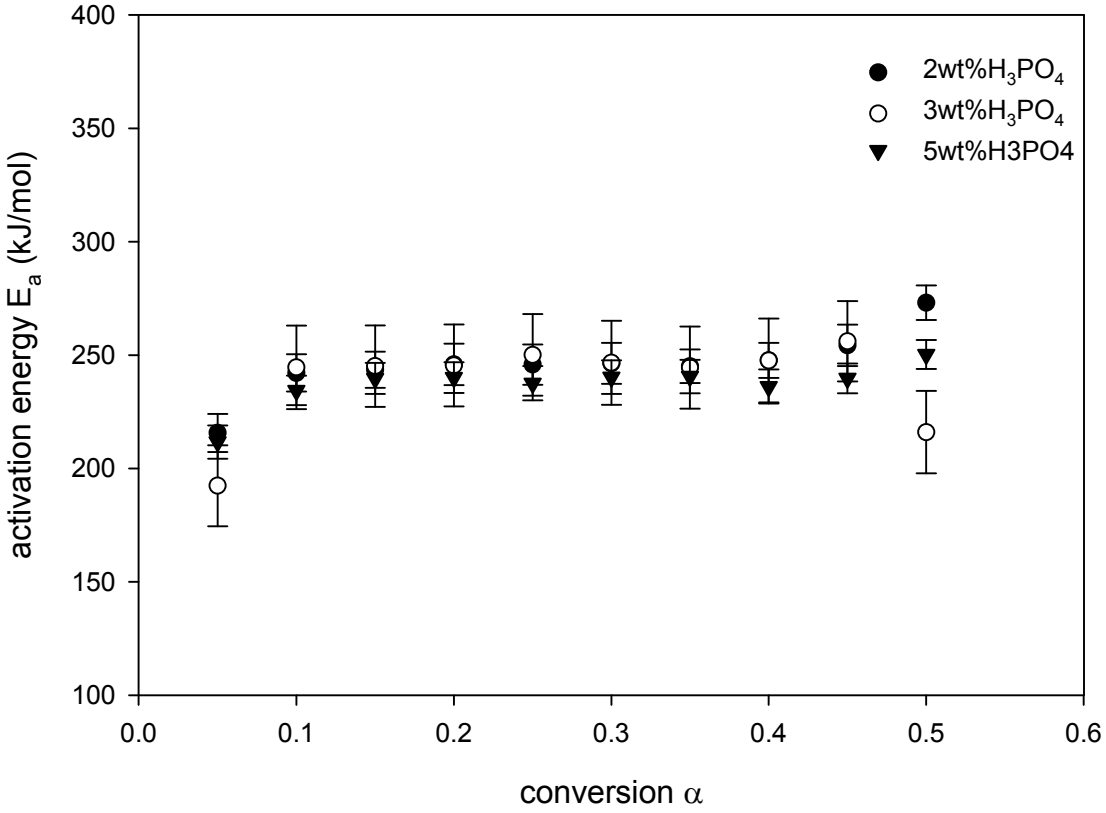

Figure 5: Variation of activation energy with conversion for cellulose degradation with various wt% H_3PO_4 added

Figure6

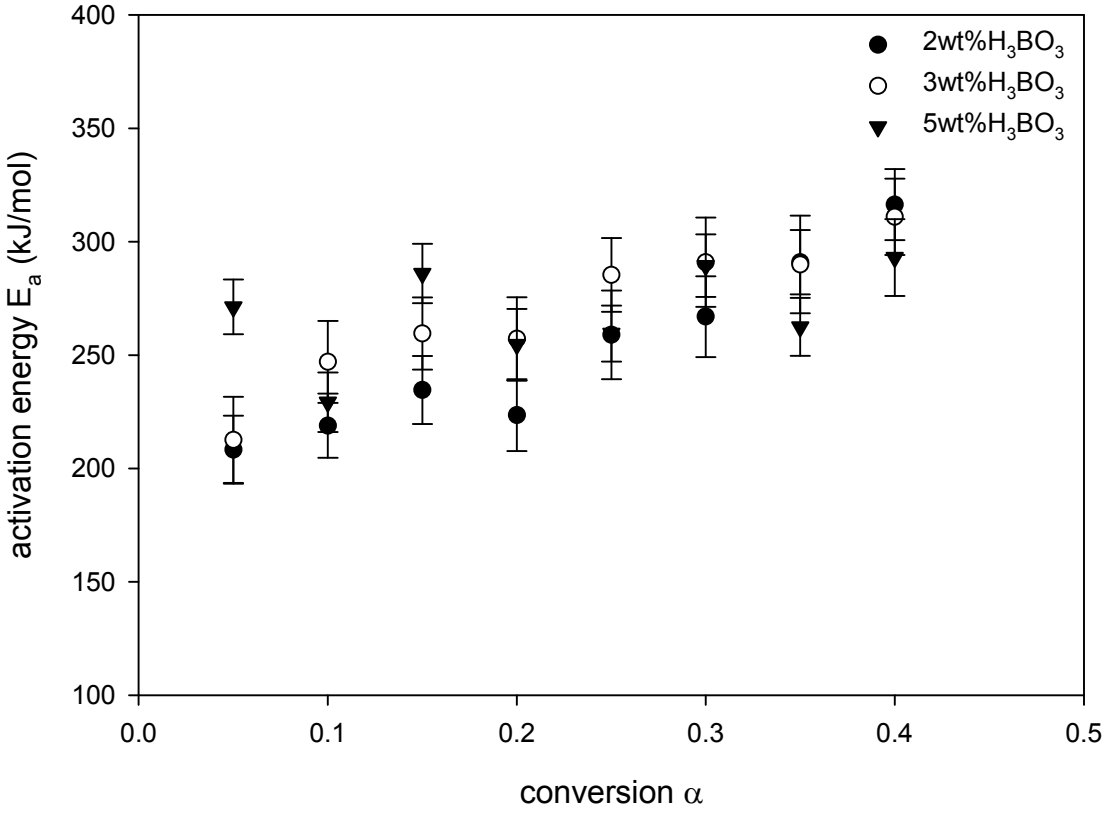

Figure 6: Variation of activation energy with conversion for cellulose degradation with various wt% H_3BO_3 added

Figure7

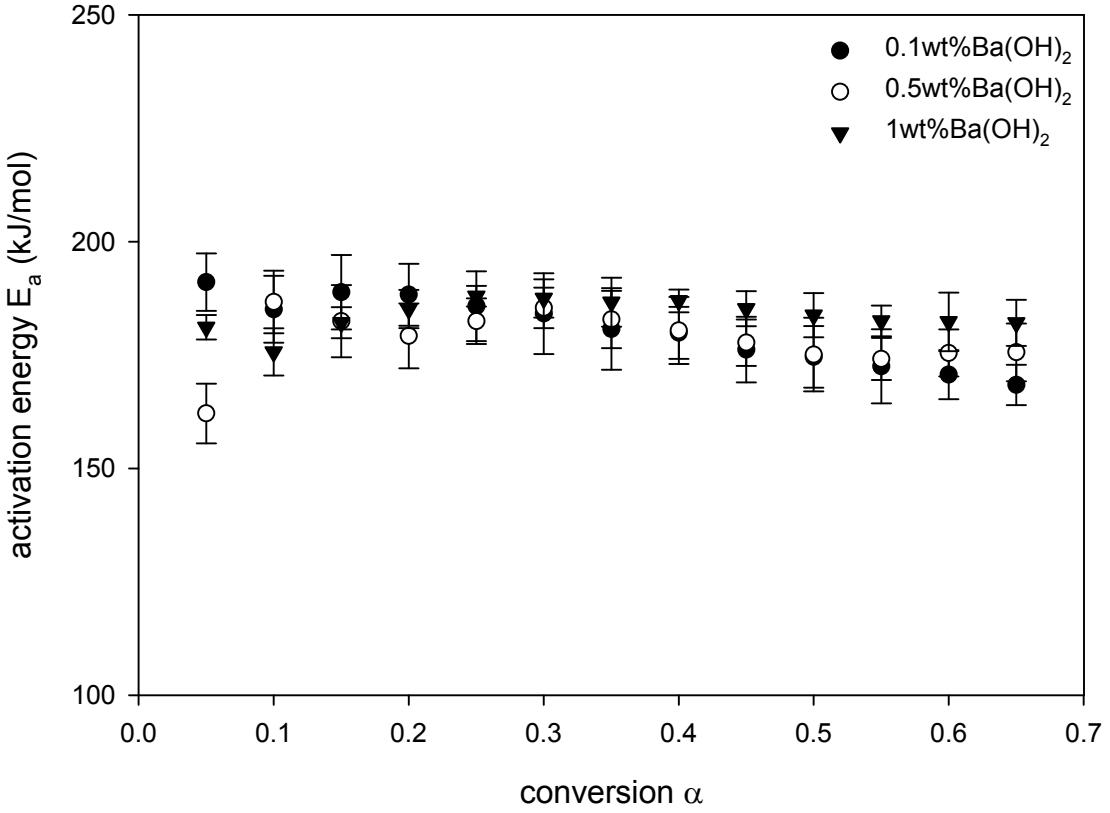

Figure 7: Variation of activation energy with conversion for cellulose degradation with various wt% $Ba(OH)_2$ added

Figure8

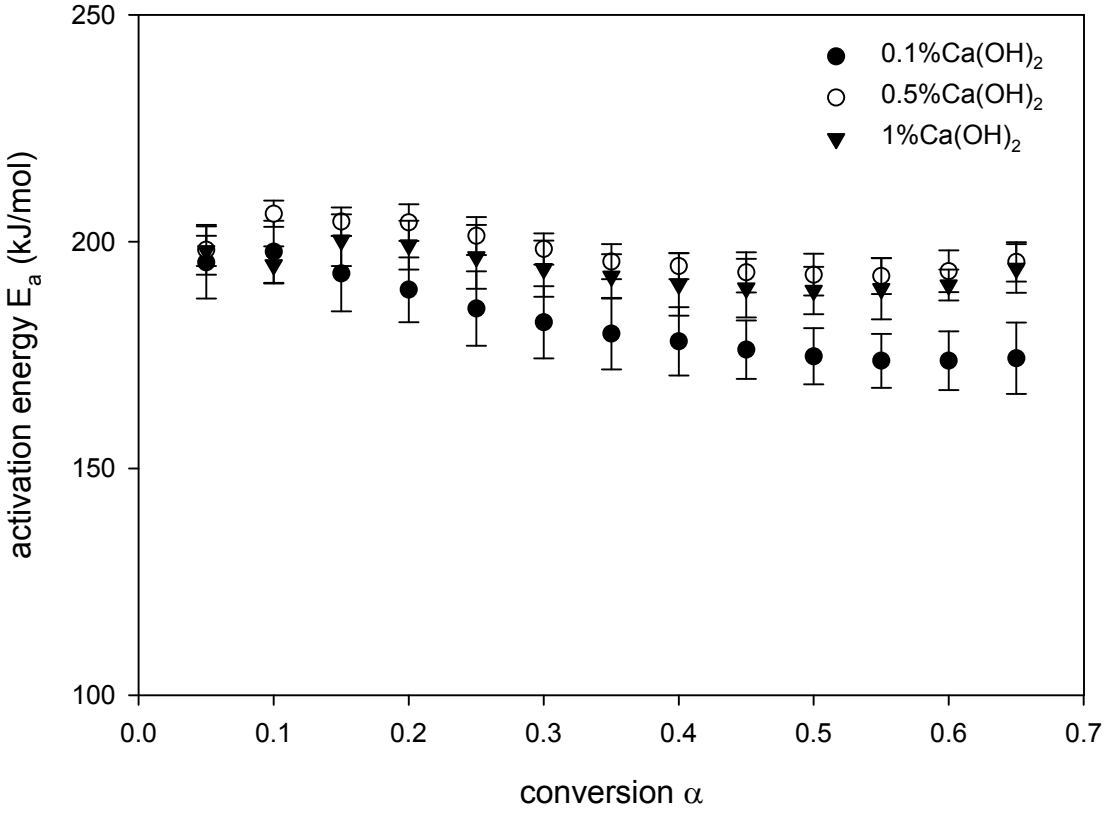

Figure 8: Variation of activation energy with conversion for cellulose degradation with various wt% $Ca(OH)_2$ added

Figure9

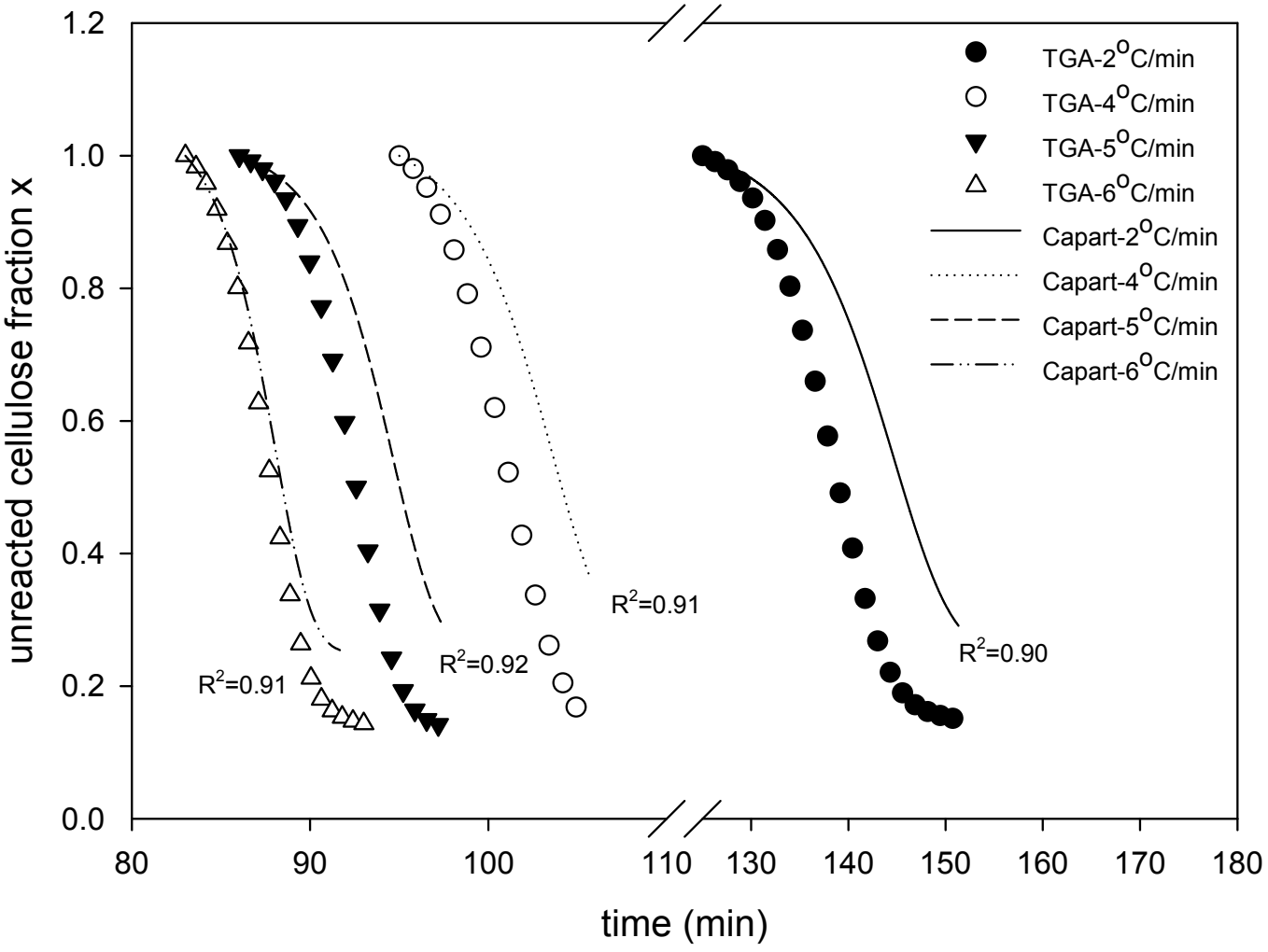

Figure 9: Comparison of Capart's model fit for pure cellulose degradation at varying heating rates.

Figure10

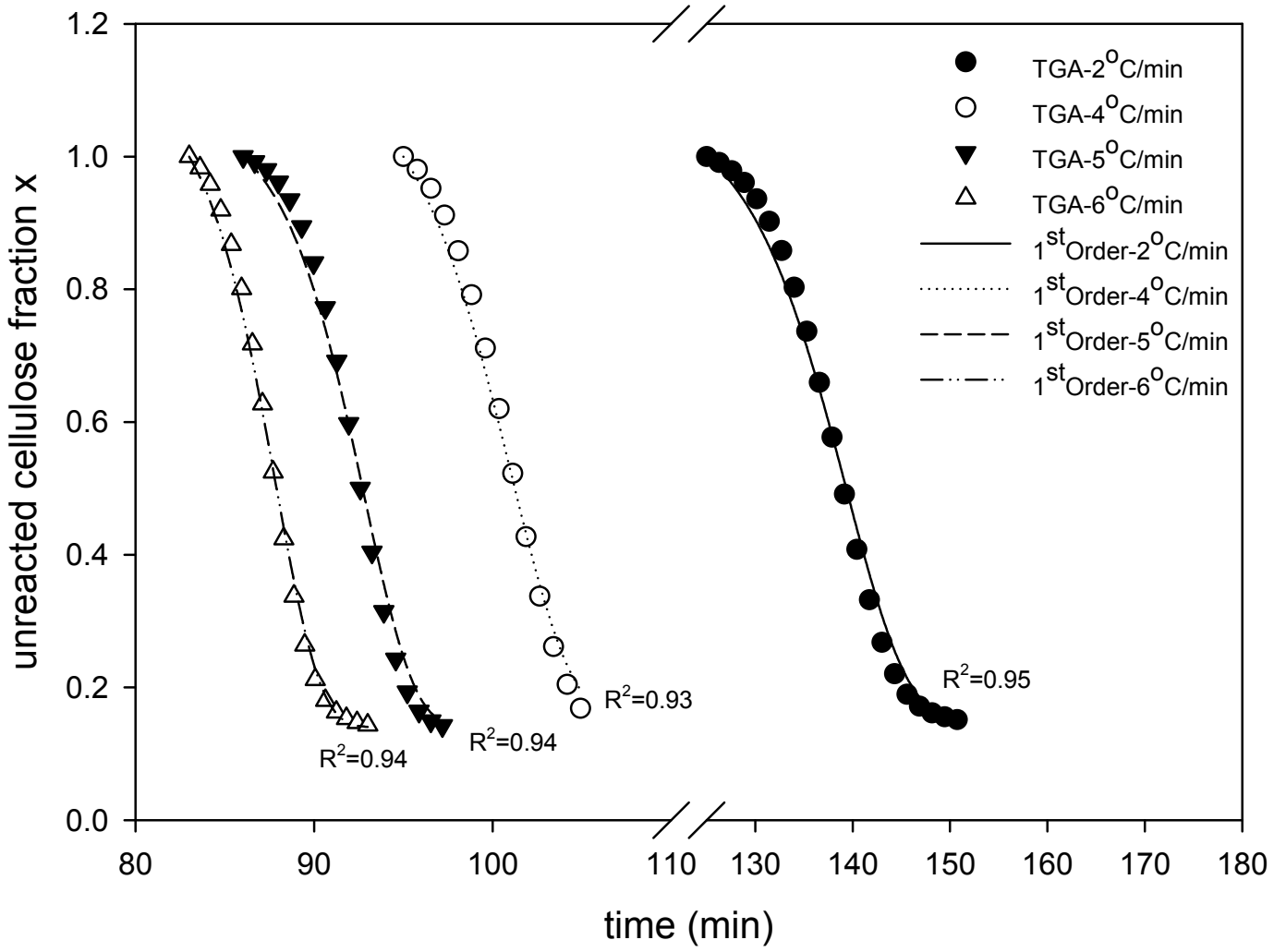

Figure 10: Comparison of first-order model fit for pure cellulose degradation at varying heating rates.

Figure11

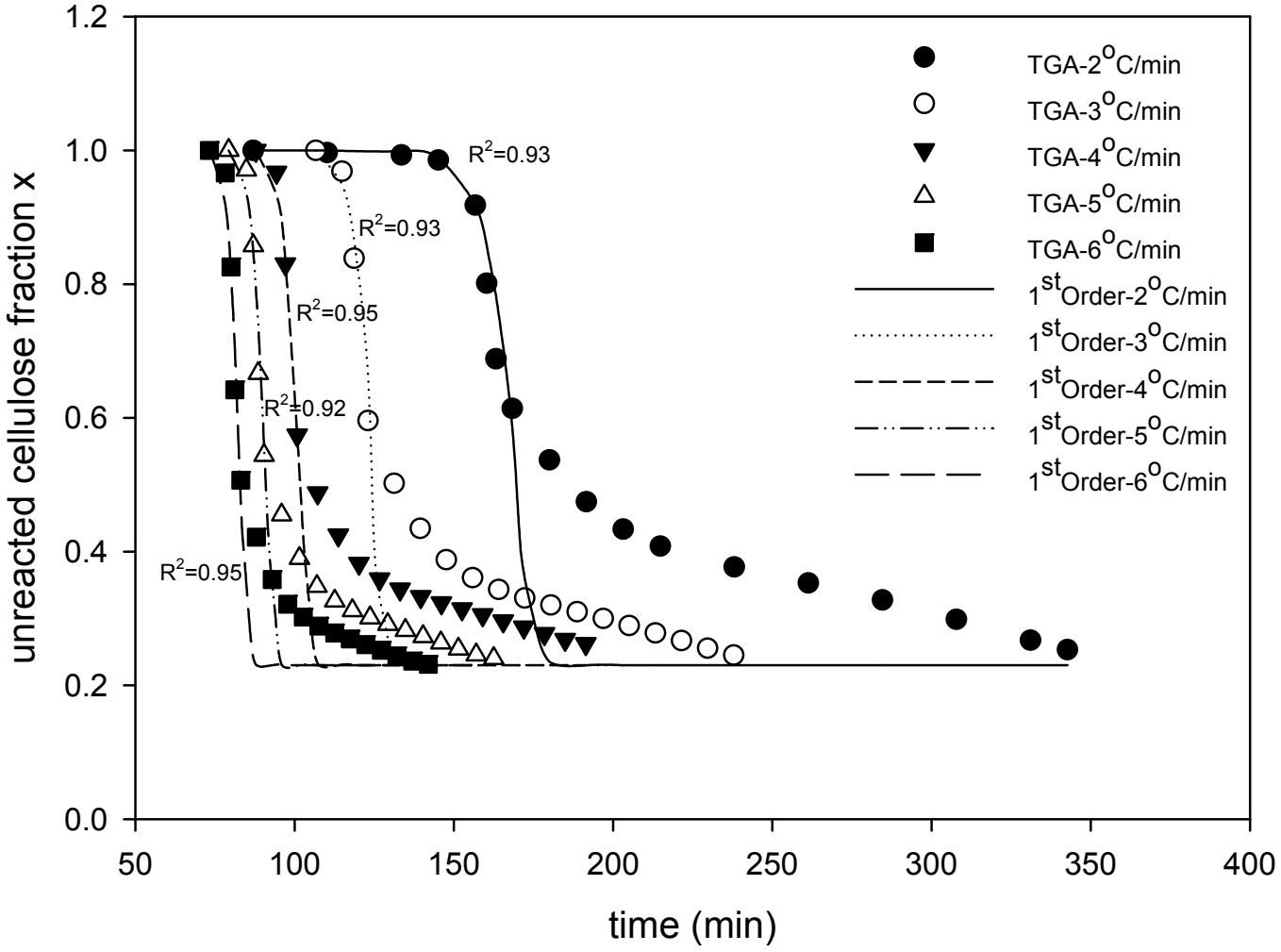

Figure 11: First-order reaction model fit of cellulose (with 2 wt% H_3PO_4) thermal degradation at various TGA heating rates (2-6 °C/min).

Figure12

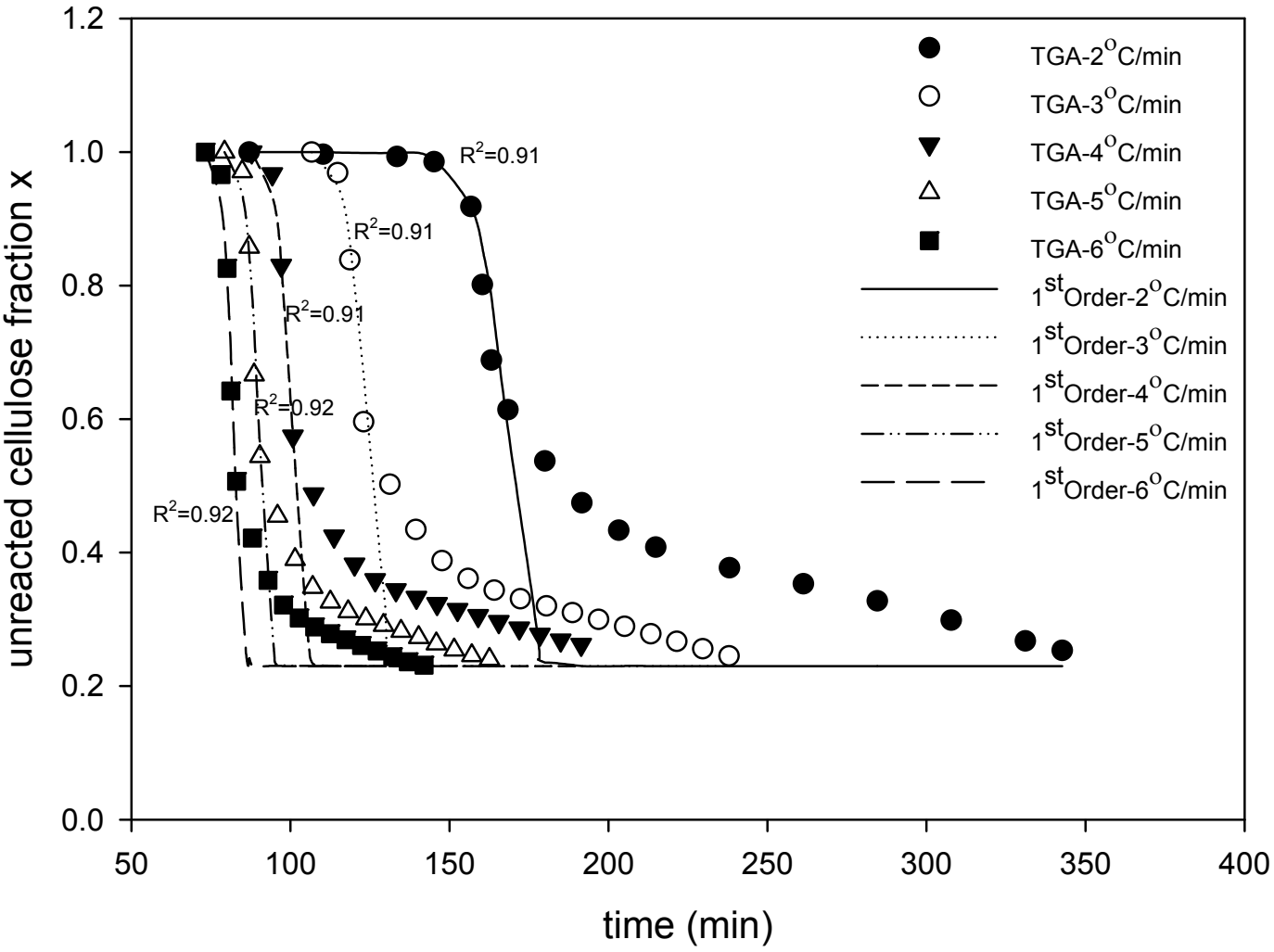

Figure 12: First-order reaction model fit of cellulose (with 2 wt% H_3BO_3) thermal degradation at various TGA heating rates (2-6 °C/min).

Figure13

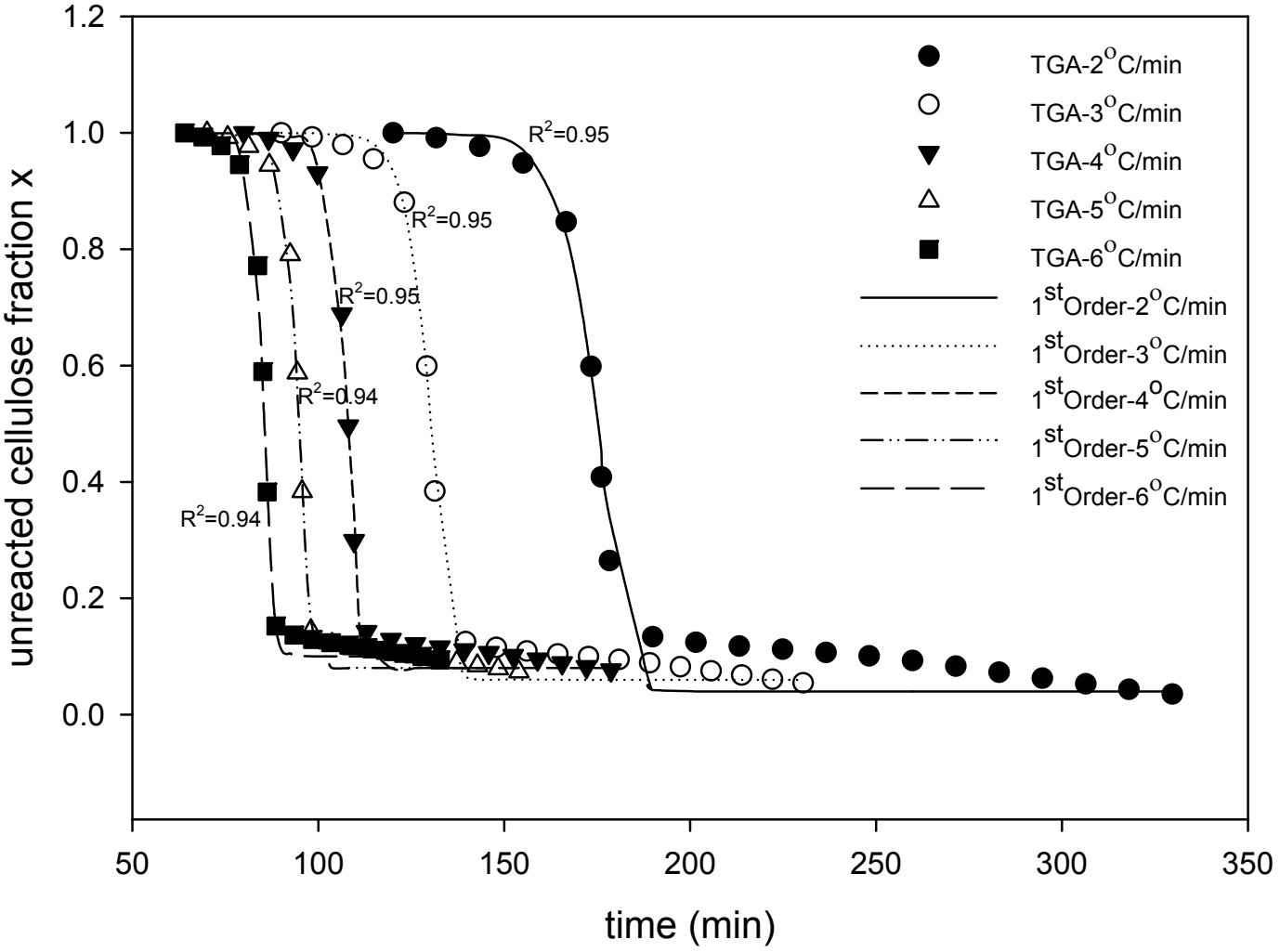

Figure 13: First-order reaction model fit of cellulose (with 0.1 wt% $Ba(OH)_2$) thermal degradation at various TGA heating rates (2-6 °C/min).

Figure14

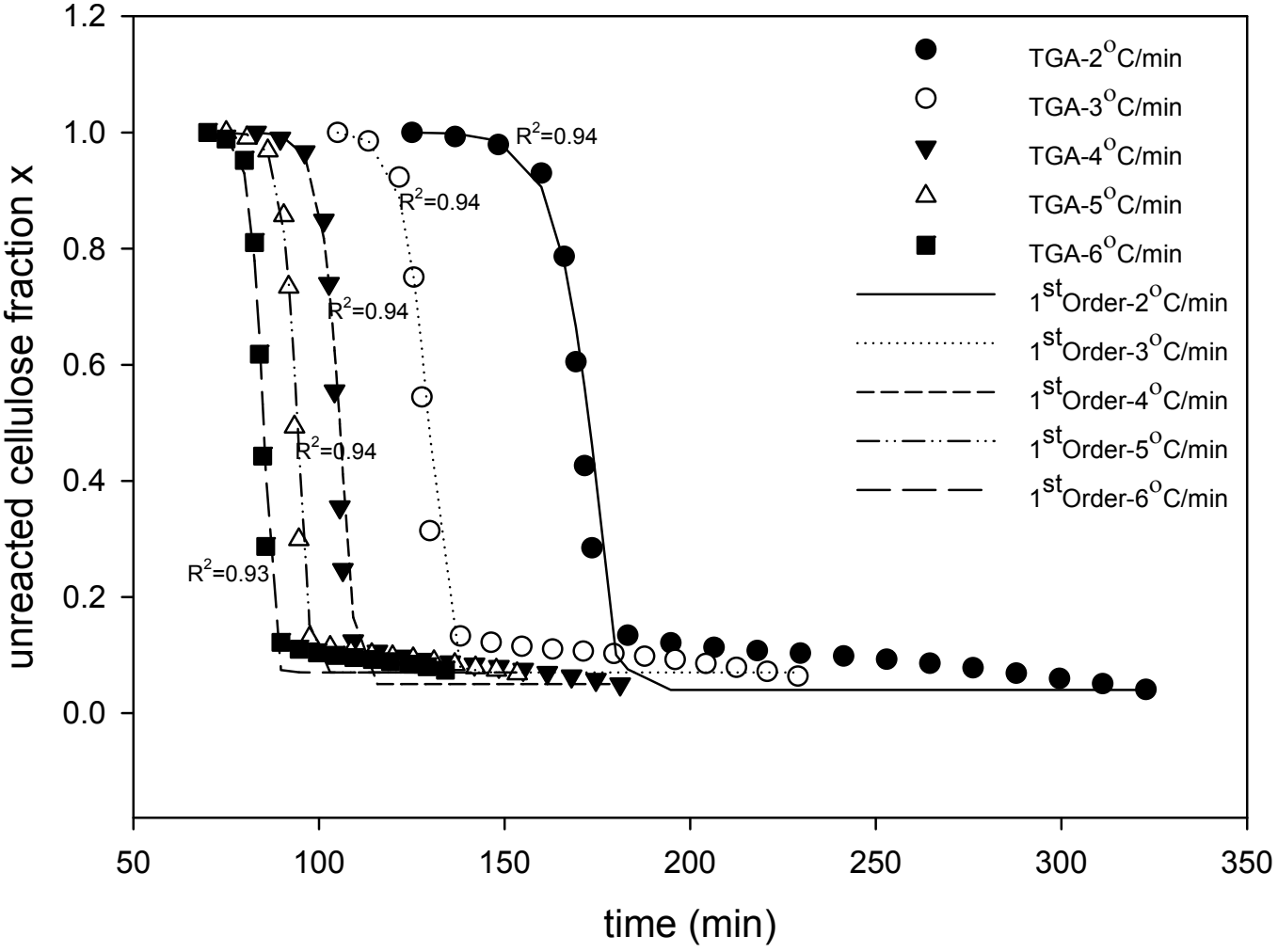

Figure 14: First-order reaction model fit of cellulose (with 0.1 wt% $Ca(OH)_2$) thermal degradation at various TGA heating rates (2-6 °C/min).